Proton-conducting oxides based on LaScO₃: structure, properties and electrochemical applications. A focus review
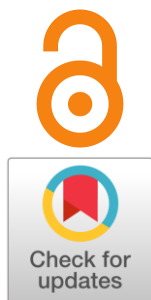
Ekaterina Antonova [a] [*]

Solid state proton conductors are promising materials for various electrochemical applications. $LaScO_3$ - based oxides are representatives of the proton-conducting oxides with perovskite structure, alternative to conventional cerates and zirconates of alkaline-earth elements. These oxides exhibit a sufficient level of proton conductivity with a combination of good chemical stability in the H_2O and CO_2 - containing atmospheres. The current review is focused on summarizing and analyzing of the currently available data on $LaScO_3$ - based oxides. The peculiarities of crystal structure and proton defect formation, aspects of synthesis and obtaining dense ceramics, and electrical properties are provided. Additionally, the current state of applications in electrochemical devices of $LaScO_3$ - based oxides is briefly discussed.

1. Introduction

Solid oxides with a perovskite structure attract the attention of researchers due to various possible applications [1–3]. One of them is solid oxide fuel cells - devices that convert chemical energy directly into electricity. A conventional SOFC consists of a solid electrolyte membrane with oxygen-ionic conductivity and two electrodes (anode and cathode) [4, 5]. To date, one of the main obstacles to the wide commercialization of SOFCs is their high working temperature (about 800 °C), which leads to a high price for electricity. Therefore, there is a demand to develop new functional materials that can operate at reduced temperatures. This can be achieved by using solid state proton conductors (SSPC) as an electrolyte membrane in SOFC instead of oxygen-ionic conductors. Since the activation energy of proton conductivity is lower than that of the oxygen-ionic, a sufficient level of conductivity can be achieved at lower temperatures (below 700 °C), thus reducing the operating temperature of the electrochemical device [6, 7]. Iwahara et al. first reported proton conductivity in complex oxides in 1981 [8]. Since that time, a huge amount of various oxides have been studied considering the possibility of proton transport in their structure, e.g. with perovskite [9–13], pyrochlore [14–17], brownmillerite and layered structures [17–20]. The most well-studied oxides are materials based on cerates and zirconates of alkaline earth elements, presenting the class of $A^{2+}B^{4+}O_3$ perovskites. They usually exhibit a high level of proton conductivity, but suffer from low chemical stability and high grain boundary resistance [21, 22]. Another group of the oxides with perovskite structure has the common formula $A^{3+}B^{3+}O_3$, such as $LaGaO_3$, $LaInO_3$, $LaScO_3$, $LaAlO_3$, etc. [23–25]. Among them, $LaScO_3$ - based oxides were found to exhibit sufficient level of proton conductivity with the combination of good chemical

a: Kinetics laboratory, Institute of High-Temperature Electrochemistry, Ekaterinburg 620066, Russian Federation

* Corresponding author: antonova_ek@list.ru

stability in the H_2O and CO_2 - containing atmospheres [23]. Therefore, these oxides can be considered as promising electrolyte materials for SOFCs or other electrochemical devices. The purpose of this paper is to provide a brief overview of the current status of studies on $LaScO_3$ - based oxides and their electrochemical applications.

2. $LaScO_3$ - based oxides: synthesis, structure, water uptake

The most common way to obtain complex oxides is a solid state reaction technique. Using this method, $LaScO_3$ - based oxides were obtained in [25–28]. However, using this method, it is difficult to obtain dense ceramics even after long-term high-temperature sintering, and therefore, the application of wet methods is necessary. Using a coprecipitaion method, $La_{1-x}Sr_xScO_{3-\delta}$ ($x = 0.01–0.2$) oxides were obtained at final sintering temperature of 1600 °C with the resulting density 94–99 % [29]. Later, Kuzmin et al. studied the influence of the synthesis technique on the resulting density of $La_{0.95}Sr_{0.05}ScO_{3-\delta}$ ceramics [30]. The solid state reaction method resulted in poor sinterability and the relative density of about 70–75 % after 10 h of sintering at 1700 °C. The combustion method with nitrates as precursors resulted in 92–96 % relative density at the same temperature. When using oxides as precursors for the combustion method, a relative density of more than 98 % was achieved after 5 h of sintering at 1650 °C [30].

Another way to obtain dense ceramic is the use of sintering aids, which have been well studied and often applied for proton conductors based on cerates and zirconates [31–34]. Few data exist for $LaScO_3$ - based oxides. Thus, the influence of the addition of CuO, ZnO, Al_2O_3, NiO, Fe_2O_3, Co_3O_4 and MoO_3 on the sinterability, microstructure, and electrical properties of $La_{0.9}Sr_{0.1}ScO_{3-\alpha}$ ceramics was studied by Kuzmin et al. [35]. The relative density of $La_{0.9}Sr_{0.1}ScO_{3-\alpha}$ tubes without sintering aids was approximately 86 %. The introduction of 1.0 wt % ZnO, Al_2O_3, NiO or 0.5–1.0 wt % Co_3O_4 leads to a relative density of ceramics higher than 95 %. The introduction of 1 wt % Fe_2O_3 additive did not affect the sinterability of the $La_{0.9}Sr_{0.1}ScO_{3-\alpha}$, and 1 wt % CuO and MoO_3 inhibited electrolyte sintering. Among dense ceramic tubes, $La_{0.9}Sr_{0.1}ScO_{3-\alpha}$ with 0.5 wt % Co_3O_4 had the highest electrical conductivity. From the other side, for $La_{1-x}Ba_xScO_{3-\alpha}$ it was observed that with an increase in the Ba content the relative density of the ceramics decreased from approximately 94 % for $x = 0.025$ to around 76 % for $x = 0.1$ [36]. In order to improve sinterability of the $La_{1-x}Ba_xScO_{3-\delta}$ oxides, Co_3O_4 was applied as a sintering additive. However, an addition of only 0.5 wt % of Co_3O_4, despite the positive sintering effect, caused a noticeable violation of stoichiometry, with partial decomposition of the material, as well as a partial substitution of Sc with Co in $La_{1-x}Ba_xScO_{3-\delta}$. Highly dense samples (98 %) were obtained only by high-temperature sintering at 1800 °C [36].

The basic compound $LaScO_3$, as well as the majority of $LaScO_3$ - based oxides, crystallize at room temperature in the perovskite structure with orthorhombic distortions, space group *Pnma*. Table 1 summarizes some data available in the literature. Only for the $La_{0.6}Ba_{0.4}ScO_3$ the cubic structure was reported [27], which is due to the larger size of the barium cation compared to lanthanum.

The main feature of SSPCs is the initial absence of protons in their structure. Protonic charge careers appear at elevated temperatures due to the interaction between oxygen vacancies in the oxide structure and water vapor according to the

$$H_2O + V_O^{\bullet\bullet} + O_O^{\times} \leftrightarrow 2OH_O^{\bullet} \qquad (1)$$

A proton is an elementary particle with a positive charge, which size is very small compared to the size of other ions in the oxide lattice. The interstitial proton is located close to oxygen and can be represented as an *OH* group occupying the oxygen site, i.e. *OH*•. The main stages of proton transport are rotational diffusion of the proton defect and the proton transfer towards the neighboring oxygen ion, that is, only the proton diffuses, while the oxygen ions remain in their crystallographic positions (Figure 1). Rotational diffusion was shown to be a fast process with low activation energy [39]. This suggests that the rate-limiting stage of proton transport in perovskites is the transfer of a proton to a neighboring oxygen ion. Therefore, its activation energy depends on the distance between oxygen ions, and their electronic state. Due to orthorhombic distortions in $LaScO_3$, oxygen positions are not equivalent, and there are preferable positions for proton localization. In [26] by powder neutron diffraction the crystal structures of 20 mol. % Sr-doped $LaScO_3$ treated in H_2O were investigated. It was found that protons are associated with the O1 oxygen (4*c*) site in the La and Sr containing mirror plane and exist in the space consists of two tilting ScO_6 octahedra. The O1 – H bond distance was found to be 1.12(2) Å at 3 K. Later, the same conclusion about preferable proton sites was done by Farlenkov et al. on the $La_{0.91}Sr_{0.09}ScO_{3-\delta}$ oxide [37].

From the Reaction 1 it is obvious that for the appearance of protonic defects the existence of the oxygen vacancies is necessary. The most common way to

Table 1 – Crystal structure parameters for LaScO₃ - based oxides at room temperature.

Composition	a, Å	b, Å	c, Å	V, Å³	Source
LaScO₃	5.7913(6)	8.0943(8)	5.6793(5)	266.23(5)	[37]
La₀.₉₆Sr₀.₀₄ScO₃₋δ	5.7886(3)	8.0996(7)	5.6808(4)	266.35(2)	[37]
La₀.₉₁Sr₀.₀₉ScO₃₋δ	5.7843(7)	8.1048(2)	5.6879(4)	266.65(8)	[37]
La₀.₉Sr₀.₁ScO₃₋δ	5.7918(9)	8.1005(3)	5.6799(5)	266.48(6)	[30]
La₀.₉₅Sr₀.₀₅ScO₃₋δ	5.749	8.031	5.629	–	[28]
La₀.₉Sr₀.₁ScO₃₋δ	5.830	8.133	5.715	–	[28]
La₀.₈₅Sr₀.₁₅ScO₃₋δ	5.829	8.132	5.711	–	[28]
La₀.₈Sr₀.₂ScO₃₋δ	5.734	8.100	5.722	–	[28]
La₀.₇₅Sr₀.₂₅ScO₃₋δ	5.738	8.110	5.736	–	[28]
La₀.₇Sr₀.₃ScO₃₋δ	5.736	8.092	5.721	–	[28]
La₀.₆Ba₀.₄ScO₂.₈	4.0931(4)	–	–	–	[27]
La₀.₉₇Ca₀.₀₃ScO₃₋δ	–	–	–	265.83	[38]
La₀.₉₅Ca₀.₀₅ScO₃₋δ	–	–	–	266.12	[38]
La₀.₉Ca₀.₁ScO₃₋δ	–	–	–	267.88	[38]
La₀.₉₅Ba₀.₀₅ScO₃₋δ	5.780	8.110	5.697	267.1	[36]
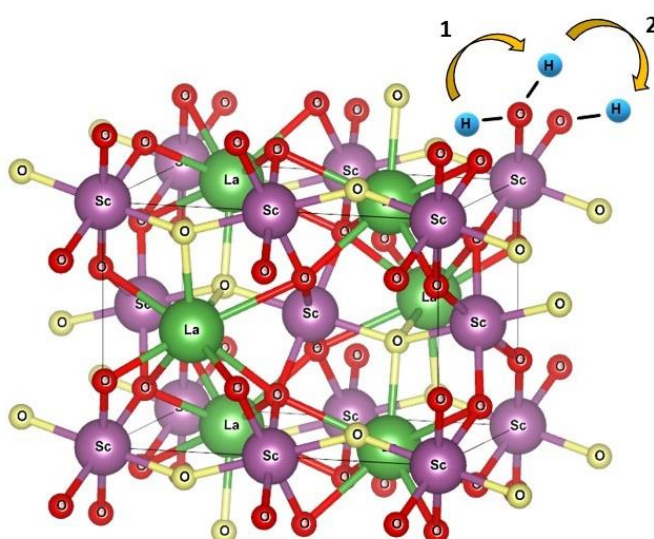
Figure 1 LaScO₃ crystal structure and the scheme of proton transport: 1) rotation diffusion; 2) proton transfer.

create oxygen vacancies is cation acceptor doping, e.g. doping with the element with lower oxidation state. In this case, oxygen vacancies are formed for keeping the electroneutrality of the crystal according to

$$MeO \xrightarrow{La_2O_3} Me'_{La} + {}^1/_2 V_O^{\cdot\cdot} + O_O^\times \qquad (2)$$
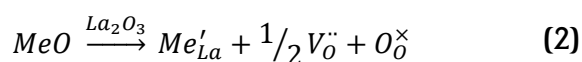
The majority of the papers are devoted to LaScO₃ - based oxides acceptor doped into La sublattice. Here, three dopants are possible: Ca, Sr, Ba. Lesnichyova et al. reported that for calcium-doped oxides, only samples with 3 and 5 mol. % of Ca were found to be single phase, while for 10 mol. % of Ca contained calcium-enriched impurity phases (according to EDX analysis), despite the fact that this sample was single-phase according to XRD [38]. On the other hand, Fujji et al. [25] presented

La₁₋ₓCaₓScO₃ (x = 0.05–0.2) as single-phase, but according only XRD data. For barium-doped oxides, Lesnichyova et al. prepared oxides with Ba content until 10 mol. %, all of them were reported to be single phase [36]. Kim et al. [27] reported La₀.₆Ba₀.₄ScO₃ to be single phase. Stroeva et al. studied doping with strontium in detail [29]. Oxides with a strontium content of up to 20 % were synthesized and all of them were found to be single phase [29]. Kato et al. [28] reported strontium solubility in LaScO₃ up to 30 mol. % of Sr.

Doping in Sc sublattice is less popular, since of the small radius of scandium. For example, Fujii et al. reported LaSc₁₋ₓMgₓO₃₋α (x = 0–0.2) to be single phase [25]. However, usually doping in Sc-sublattice is carried out in conjunction with doping the lanthanum sublattice, most often with strontium. Stroeva et al. prepared La₁₋ₓSrₓSc₁₋ᵧMgᵧO₃₋α (0.01 ≤ x = y ≤ 0.20) oxides, all of them were found to be single phase [40]. Kato et al. found that the presence of a small amount of aluminum in Sc-sublatice in La₁₋ₓSrₓSc₁₋ᵧAlᵧO₃₋δ (y = 0.01–0.05) led to the stabilization of the crystal structure suppressing phase transitions [28].

Because the formation of protonic defects according to Reaction 1 is accompanied by a significant weight increase, the concentration of protonic defects as a function of temperature and water partial pressure is usually measured by thermal gravimetric analysis (TGA). Additionally, from TGA data, thermodynamic parameters, such as enthalpy and entropy of hydration process can be estimated. Figure 2 compares results on proton concentration in LaScO₃ - based oxides available in literature. Generally, according to Equation 1, the value of maximum water uptake (saturation level) has to be

Table 2 – Hydration enthalpy ΔH_{hydr} and entropy ΔS_{hydr} values for proton conducting oxides.

Composition	ΔH_{hydr}, kJ · mol^{-1}	ΔS_{hydr}, J · mol^{-1} · K^{-1}	Experimental conditions		Source
			T, °C	pH$_2$O, atm	
La$_{0.96}$Sr$_{0.04}$ScO$_{3-\delta}$	-61 ± 5	-88 ± 5	300–950	0.24	[37]
La$_{0.91}$Sr$_{0.09}$ScO$_{3-\delta}$	-97 ± 5	-112 ± 5			
La$_{0.9}$Sr$_{0.1}$ScO$_{3-\delta}$	-105 ± 9	-116 ± 9	285–1200	0.019	[41]
La$_{0.95}$Ca$_{0.04}$ScO$_{3-\delta}$	-132 ± 5	-126 ± 5	300–950	0.24	[38]
La$_{0.95}$Ba$_{0.05}$ScO$_{3-\delta}$	-85 ± 6	-106 ± 6	300–950	0.24	[36]
BaZr$_{0.9}$Y$_{0.1}$O$_{3-\delta}$	-79.4	-88.8	500–900	0.02	[43]
BaCe$_{0.9}$Y$_{0.1}$O$_{3-\delta}$	-163.3	-167.9	600–850	0.02	[39]
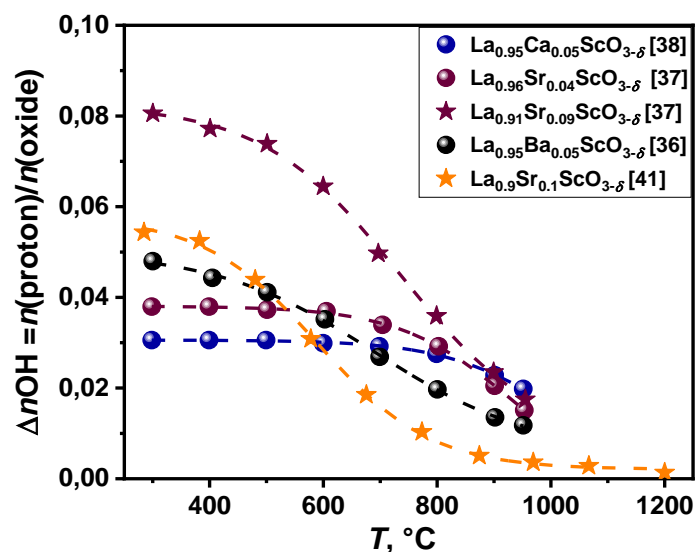
Figure 2 Temperature dependencies of proton concentration in LaScO$_3$ - based oxides.

equal to the acceptor doping concentration. One can see that for LaScO$_3$ - based oxides exact match between the saturation level n_{OH} and the acceptor concentration x is not observed. This phenomenon is often explained by the existence of a strong bond of the acceptor defects with oxygen vacancies, which do not participate in the hydration process [41]. In the case of LaScO$_3$ - based oxides, this phenomenon can be associated with oxygen vacancies not fully filled due to non-equality of O1 and O2 oxygen positions [26, 42].

Table 2 gives a comparison of the thermodynamic parameters of the hydration process for LaScO$_3$ - based oxides. The values are comparable with those for the best-known proton conducting oxides based on cerates and zirconates [39, 43].

3. Electrical properties

Generally, LaScO$_3$ - based oxides in an oxidizing atmosphere exhibit mixed oxygen-ionic, proton and hole conductivity, and in reducing conditions they exhibit pure ionic conductivity (mixed oxygen-ionic and proton). The contributions of different types of conductivity strongly depend on external conditions such as

temperature, oxygen and water vapor partial pressures, and the pure proton conductivity is usually observed at temperatures below 500 °C in reducing atmospheres.

Several works studied the influence of the level of doping and type of dopant on the electrical conductivity of the LaScO$_3$ - based oxides. Thus, Stroeva et al. studied the electrical conductivity of La$_{1-x}$Sr$_x$Sc$_{1-y}$Mg$_y$O$_{3-\delta}$ ($x = y = 0.01$–0.2) in different atmospheres [40, 44]. Only a slight change in conductivity depending on the concentration of dopants was observed. As the temperature decreases, the maximum in the concentration dependencies of conductivity shifts to side of smaller additions of Sr and Mg. Lybye et al. compared the electrical conductivity data of La$_{0.9}$Sr$_{0.1}$ScO$_{3-\delta}$ and La$_{0.9}$Sr$_{0.1}$Sc$_{0.9}$Mg$_{0.1}$O$_{3-\delta}$ and concluded that in the case of LaScO$_3$ - based materials, Sr doping only in the A-sublattice is more effective than double doping of Sr and Mg in A and B-sublattice respectively [24]. The authors associate the decrease in the electrical conductivity of La$_{0.9}$Sr$_{0.1}$Sc$_{0.9}$Mg$_{0.1}$O$_{3-\delta}$ with the segregation of MgO at the grain boundaries, which they observed when studying samples using transmission electron microscopy. A decrease in bulk ionic conductivity and proton transfer numbers was also noted for La$_{0.9}$Sr$_{0.1}$Sc$_{0.9}$Mg$_{0.1}$O$_{3-\delta}$ compared to La$_{0.9}$Sr$_{0.1}$ScO$_{3-\delta}$ [45].

As follows from Reaction 2, the concentration of oxygen vacancies is proportional to the concentration of the dopant. Nevertheless, conductivity usually has a maximum at a certain dopant concentration and begins to decrease with its further increase since charged defects begin to interact with each other, leading to a decrease in their mobility [46]. Thus, for Sr-doped LaScO$_3$, despite the high Sr solubility in LaScO$_3$, the maximum of the electrical conductivity is observed for La$_{0.9}$Sr$_{0.1}$ScO$_{3-\delta}$ [45]. As dopants for the A-position, Ca, Sr, and Ba were studied [36, 38, 47]. Figure 3 compares electrical conductivity values for A-site doped LaScO$_3$ in air and reductive conditions. The temperature dependencies in reductive conditions demonstrate an inflection caused by the superposition of two types of ion transfer, i.e. oxygen ions
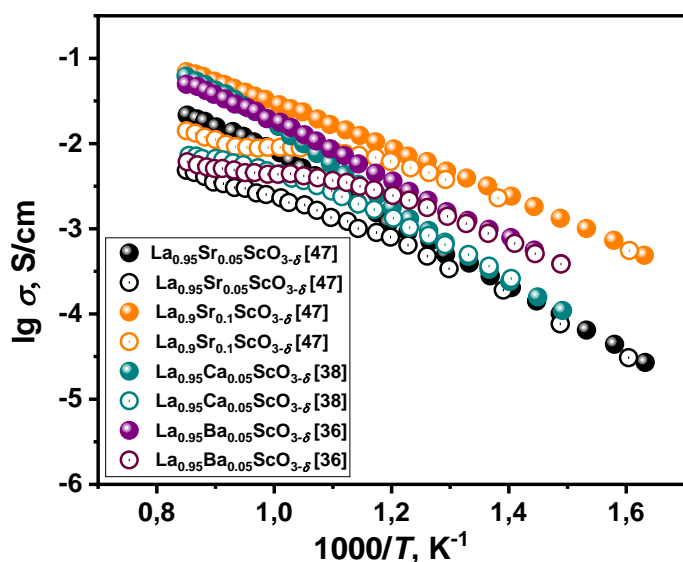
Figure 3 Temperature dependencies of the electrical conductivity for LaScO$_3$ - based oxides in air (filled symbols) and reductive (empty symbols) atmospheres.

at higher temperatures and protons at lower ones. Conductivity values in oxidizing and reducing atmospheres are close at temperatures below 500 °C, which indicates a low level of hole conductivity in air conditions, while at high temperatures they vary greatly due to the significant contribution of hole conductivity. Belyakov et al. using the pair distribution function and photoluminescence revealed the features of the crystal and electronic structures for La$_{0.95}$M$_{0.05}$ScO$_{3-\delta}$ (M = Ca, Sr, Ba) and studied the influence of the dopant on the hydration ability and electrical conductivity of the oxide [48]. They showed that the dopant-induced local distortions in the crystal structure and the electronic structure of the material influence the hydration process. Strontium was found to be the optimal dopant due to the combination of high proton stability and mobility. In summary, the best combination of doping level, electrical conductivity, phase stability and mechanical properties is observed for 10 mol. % Sr-doped LaScO$_3$.

Since that for electrochemical application polycrystal materials are applied, it is important to know the contributions of bulk and grain boundaries to the total resistance of the ceramics. These data can be obtained by impedance spectroscopy measurements. It is well known that the bulk resistance is an intrinsic property of the material, determined by chemical composition and crystal structure. In contrast, grain boundary conductivity can differ in a wide range depending on different techniques of sample preparation, purity of the starting reagents, etc., resulting in different microstructure (grain size, purity of grain boundaries, porosity). Kuzmin et al. compared bulk and grain boundary conductivities of

5 mol. % Sr-doped LaScO$_3$ ceramics obtained by three different methods with different porosity and grain size [30]. It was found that bulk conductivities and their activation energy in the air atmosphere did not depend on the density of the samples. Activation energy of grain boundary and bulk conductivities were almost identical for the samples with 94 % and 98 % densities, while for the sample with 70 % density it was sufficiently higher. The authors conclude that for the samples with low porosity, there are no additional barriers for charge carriers on the grain boundaries compared to the charge transfer in the bulk, and the lower grain boundary conductivity is caused by fewer carriers crossing the grain boundaries. The bridge model on semi-coherent boundaries i.e. such boundaries, when only a part of atomic lattice planes of one grain continues in the lattice of another grain is proposed for explaining a low grain boundary conductivity. Such a boundary in a solid electrolyte accumulates complex defects: clusters of point defects, nanopores, and impurities. With increasing the porosity of the sample, the concentration of such defects increases and the semi-coherent boundary becomes incoherent with low conductivity and high activation energy, which is observed for the sample with 70 % density. Since the LaScO$_3$ - based oxides have a non-cubic lattice, it is impossible to reach high boundary coherence even for high-density samples, therefore, such materials will always exhibit higher grain boundary resistance compared to the bulk one. In order to get rid of low conducting boundaries, these materials should be used in the form of pseudo monocrystalline films, i.e. films with a grain size not less than its thickness.

4. Applications in the electrochemical devices

La$_{0.675}$Sr$_{0.325}$Sc$_{0.99}$Al$_{0.01}$O$_3$ was applied as an electrolyte membrane in an electrolyte-supported fuel cell in [49]. Using Pt, Ni-YSZ Ni-SDC as anodes, and Pt or La$_{0.8}$Sr$_{0.2}$MnO$_3$ as cathodes, the resulting power density was 47 mW · cm^{-2} when the cathode and anode were both platinum. At 1000 °C, the maximum power density was 158 mW · cm^{-2} with humidified hydrogen fuel using Ni-SDC and LSM as the anode and cathode, respectively. Further, the same authors manufactured and tested anode-supported fuel cell on the NiO–8YSZ substrate [50]. (La$_{0.675}$Sr$_{0.325}$)(Sc$_{0.98}$Co$_{0.02}$)O$_{3-\delta}$ thin film was deposited onto the substrate by pulsed laser deposition method, Pt was applied as a cathode. However, very low power densities were obtained: 21.6, 8.8, 3.5, and 1.9 mW · cm^{-2} at 780, 700, 650, and 600 °C, respectively. It was suggested that both the low electrical performances in the electrolyte and the unsuitable electrodes were responsible for this poor performances.

Plekhanov et al. made an attempt to modify $La_{0.9}Sr_{0.1}ScO_{3-\delta}$ electrolyte by transition metals and apply the obtained oxides as an electrolyte component in composite electrodes for $La_{0.9}Sr_{0.1}ScO_{3-\delta}$ [51]. It was shown that $La_{0.9}Sr_{0.1}Sc_{0.9}Co_{0.1}O_{3-\delta}$ has the highest value of conductivity among other compositions. A single fuel cell $La_{0.9}Sr_{0.1}Sc_{0.9}Co_{0.1}O_{3-\delta} - LaFe_{0.6}Ni_{0.4}O_3 \mid La_{0.9}Sr_{0.1}ScO_{3-\delta} \mid La_{0.9}Sr_{0.1}Sc_{0.9}Co_{0.1}O_{3-\delta}$-Ni was tested and the maximum power density of the cell reached $35.5\ mW \cdot cm^{-2}$ at 800 °C. The authors consider high electrolyte resistance to be the main obstacle for better performance. Nevertheless, the fuel cell with $La_{0.9}Sr_{0.1}Sc_{0.9}Co_{0.1}O_{3-\delta}$ in both electrodes has significantly better performance compared to the cell with $La_{0.9}Sr_{0.1}ScO_{3-\delta}$ component in the electrodes, which had a maximum power density of $0.14\ mW \cdot cm^{-2}$ at 800 °C. Kuzmin et al. obtained close result of $30\ mW \cdot cm^{-2}$ for a single tubular fuel cell made on a supporting $La_{0.9}Sr_{0.1}ScO_{3-\delta}$ electrolyte with the same electrodes [35]. Finally, in recent work, Osinkin et al. tested an electrochemical cell based on $La_{0.9}Sr_{0.1}ScO_{3-\delta}$ electrolyte as a hybrid setup for electricity generation in the proton ceramic fuel cell mode, for hydrogen separation from the $H_2 + Ar$ mixture and the production of high-purity hydrogen from methane with simultaneous CO_2 utilization [52]. Symmetrical $Sr_{1.95}Fe_{1.4}Ni_{0.1}Mo_{0.5}O_{6-\delta} + La_{0.9}Sr_{0.1}Sc_{0.9}Co_{0.1}O_{3-\delta}$ composite electrodes were applied on the supporting $La_{0.9}Sr_{0.1}ScO_{3-\delta}$ electrolyte. In the fuel cell mode, the same values of the power density of about $33\ mW \cdot cm^{-2}$ were obtained, suggesting that regardless of the activity of the electrodes, the ohmic resistance of the supporting electrolyte primarily determines the power of such a cell. Another possible reason for not achieving high power density values is the presence of electronic (hole) conductivity in the $La_{0.9}Sr_{0.1}ScO_{3-\delta}$ supporting electrolyte on the side of the oxidizing atmosphere, leading to a decrease in the cell power due to the the leakage current. In the mode of hydrogen separation through a proton-conducting membrane from an $H_2 + Ar$ mixture, a flow rate of hydrogen about of $500\ cm^3 \cdot h^{-1} \cdot cm^{-2}$ at a current density of $0.6\ A \cdot cm^{-2}$ was obtained at 800 °C. During the hydrogen separation from methane and carbon dioxide mixture at a current density of $0.5\ A \cdot cm^{-2}$, the hydrogen flow rate was about $370\ cm^3 \cdot h^{-1} \cdot cm^{-2}$ at 800 °C, which shows that these cells are promising for hydrogen production.

5. Conclusions

Solid state proton conductors are of great interest due to their possible application in the solid state electrochemical devices working in the medium-temperature range (500–700 °C). Among them, $LaScO_3$ - based oxides are promising candidates, competing with well-known zirconates and cerates of alkaline-earth elements due to the combination of a sufficient level of proton conductivity with good chemical stability in the H_2O and CO_2 - containing atmospheres. The structural and functional properties of various $LaScO_3$ - based oxides are already well studied, and the most promising composition is found to be 10 mol. % oped $LaScO_3$. Several attempts have been made to apply this electrolyte in electrochemical cells, and promising results have been obtained. However, there are still several issues that need to be resolved. It is necessary to develop technologies for obtaining dense thin films in order to decrease the ohmic resistance of the cells, with special attention to obtain large grains for decreasing the grain boundary resistance. Another obstacle is the presence of hole conductivity in the electrolyte at high temperatures, and therefore, a decrease in cell performance due to the leakage current. This can be overcome by decreasing the operating temperatures of the electrochemical devices up to 500–600 °C, where the contribution of hole conductivity in the electrolyte is less pronounced. However, in this case, the problem of suitable electrodes efficiently operating at such temperatures arises.

Supplementary materials

No supplementary materials are available.

Funding

Acknowledgments

Author contributions

Ekaterina Antonova: Conceptualization; Writing – Original draft; Writing – Review & Editing; Visualization.

Conflict of interest

The authors declare no conflict of interest.

Additional information

Ekaterina Antonova, PhD, senior researcher, Kinetics laboratory; Institute of High Temperature Electrochemistry Ural Branch of Russian Academy of Science, Ekaterinburg, Russian Federation; ORCID: 0000-0003-3902-4395; Web of Science Reseacher ID: H-9313-2016.

References

1. Mohan M, Shetti NP, Aminabhavi TM, Perovskites: A new generation electrode materials for storage applications, J. Power Sources, **574** (2023) 233166. https://doi.org/10.1016/j.jpowsour.2023.233166

2. Jiang X, Yin WJ, High-throughput computational screening of oxide double perovskites for optoelectronic and photocatalysis applications, J. Energy Chem., **57** (2021) 351–358. https://doi.org/10.1016/j.jechem.2020.08.046

3. Mahmoudi F, Saravanakumar K, Maheskumar V, Njaramba LK, et al., Application of perovskite oxides and their composites for degrading organic pollutants from wastewater using advanced oxidation processes: Review of the recent progress, J. Hazard. Mater., **436** (2022) 129074. https://doi.org/10.1016/j.jhazmat.2022.129074

4. Golkhatmi SZ, Asghar MI, Lund PD, A review on solid oxide fuel cell durability: latest progress, mechanisms, and study tools, Renew. Sustain. Energy Rev., **161** (2022) 112339. https://doi.org/10.1016/j.rser.2022.112339

5. Mahato N, Banerjee A, Gupta A, Omar S, Balani K, Progress in material selection for solid oxide fuel cell technology: A review, Prog. Mater. Sci., **72** (2015) 141–337. http://dx.doi.org/10.1016/j.pmatsci.2015.01.001

6. Fabbri E, Bi L, Pergolesi D, Traversa E, Towards the next generation of solid oxide fuel cells operating below 600 °C with chemically stable proton-conducting electrolytes, Adv. Mater., **24** (2012) 195–208. https://doi.org/10.1002/adma.201103102

7. Kim J, Sengodan S, Kim S, Kwon O, et al., Proton conducting oxides: a review of materials and applications for renewable energy conversion and storage, Renew. Sust. Energ. Rev., **109** (2019) 606–618. https://doi.org/10.1016/j.rser.2019.04.042

8. Iwahara H, Esaka T, Uchida H, Maeda N, Proton conduction in sintered oxides and its application to steam electrolysis for hydrogen production, Solid State Ionics, **3–4** (1981) 359–363. https://doi.org/10.1016/0167-2738(81)90113-2

9. Medvedev D, Murashkina A, Pikalova E, Demin A, et al., BaCeO$_3$: materials development, properties and application, Prog. Mater. Sci., **60** (2014) 72–129. https://doi.org/10.1016/j.pmatsci.2013.08.001

10. Hossain MK, Chanda R, El-Denglawey A, Emrose T, et al., Hashizume K, Recent progress in barium zirconate proton conductors for electrochemical hydrogen device applications: A review, Ceramics Int., **47** (2021) 23725–23748. https://doi.org/10.1016/j.ceramint.2021.05.167

11. Liu Y, Ran R, Tade MO, Shao Z, Structure, sinterability, chemical stability and conductivity of proton-conducting BaZr$_{0.6}$M$_{0.2}$Y$_{0.2}$O$_{3-\delta}$ electrolyte membranes: the effect of the M dopant, J. Membr. Sci., **467** (2014) 100–108. https://doi.org/10.1016/j.memsci.2014.05.020

12. Zvonareva IA, Medvedev DA, Proton-conducting barium stannate for high-temperature purposes: A brief review, J. Eur. Ceram. Soc., **43** (2023) 198–207. https://doi.org/10.1016/j.jeurceramsoc.2022.10.049

13. Li H, Li Y, Huang W, Ding Y, Effect of various doping on electrochemical properties of KNbO$_3$ proton conductor, Solid State Ionics, **399** (2023) 116318. https://doi.org/10.1016/j.ssi.2023.116318

14. Shlyakhtina AV, Abrantes JCC, Gomes E, Lyskov NV, et al., Evolution of oxygen–ion and proton conductivity in Ca-doped Ln$_2$Zr$_2$O$_7$ (Ln = Sm, Gd), located near pyrochlore–fluorite phase boundary, Materials, **12** (2019) 2452. https://doi.org/10.3390/ma12152452

15. Zhu Z, Liu B, Shen J, Lou Y, Ji Y, La$_2$Ce$_2$O$_7$: A promising proton ceramic conductor in hydrogen economy, J. Alloys Compd., **659** (2016) 232–239. https://doi.org/10.1016/j.jallcom.2015.11.041

16. Antonova EP, Farlenkov AS, Tropin ES, Eremin VA, et al., Oxygen isotope exchange, water uptake and electrical conductivity of Ca-doped lanthanum zirconate, Solid State Ionics, **306** (2017) 112–117. https://doi.org/10.1016/j.ssi.2017.03.023

17. Fop S, Solid oxide proton conductors beyond perovskites, J. Mater. Chem. A, **9** (2021) 18836. https://doi.org/10.1039/d1ta03499e

18. Tarasova NA, Animitsa IE, Galisheva AO, Medvedev DA, Layered and hexagonal perovskites as novel classes of proton-conducting solid electrolytes. A focus review, Electrochem. Mater. Technol., **1** (2022) 20221004. https://doi.org/10.15826/elmattech.2022.1.004

19. Tarasova N, Galisheva A, Animitsa I, Korona D, Davletbaev K, Novel proton-conducting layered perovskite based on BaLaInO$_4$ with two different cations in B-sublattice: synthesis, hydration, ionic (O^{2-}, H$^+$) conductivity, Int. J. Hydrog. Energy, **47** (2022) 18972–18982. https://doi.org/10.1016/j.ijhydene.2022.04.112

20. Tarasova N, Bedarkova A, Animitsa I, Abakumova E, et al., Novel protonic conductor SrLa$_2$Sc$_2$O$_7$ with layered structure for electrochemical devices, Materials, **15** (2022) 8867. https://doi.org/10.3390/ma15248867

21. Rashid NLRM, Samat AA, Jais AA, Somalu MR, et al., Review on zirconate-cerate-based electrolytes for proton-conducting solid oxide fuel cell, Ceramics Int., **45** (2019) 6605–6615. https://doi.org/10.1016/j.ceramint.2019.01.045

22. Antonova EP, Yaroslavtsev IYu, Bronin DI, Balakireva VB, et al., Peculiarities of electrical transfer and isotopic effects H/D in the proton–conducting oxide BaZr$_{0.9}$Y$_{0.1}$O$_{3-\delta}$, Russ. J. Electrochem., **46** (2010) 741–748. https://doi.org/10.1134/S1023193510070049

23. Nomura K, Takeuchi T, Tanase S, Kageyama H, et al., Proton conduction in (La$_{0.9}$Sr$_{0.1}$)M^{III}O$_{3-\delta}$ (M^{III}=Sc, In, and Lu)

perovskites, Solid State Ionics, **154–155** (2002) 647–652. https://doi.org/10.1016/S0167-2738(02)00512-X

24. Lybye D, Poulsen FW, Mogensen M, Conductivity of A- and B-site doped LaAlO$_3$, LaGaO$_3$, LaScO$_3$ and LaInO$_3$ perovskites, Solid State Ionics, **128** (2000) 91–103. https://doi.org/10.1016/S0167-2738(99)00337-9

25. Fujii H, Katayama Y, Shimura T, Iwahara H, Protonic conduction in perovskite-type oxide ceramics based on LnScO$_3$ (Ln=La, Nd, Sm or Gd) at high temperature, J Electroceram., **2** (1998) 119–125. https://doi.org/10.1023/A:1009935208872

26. Nomura K, Kageyama H, Neutron diffraction study of LaScO$_3$-based proton conductor, Solid State Ionics, **262** (2014) 841–844. http://dx.doi.org/10.1016/j.ssi.2013.09.018

27. Kim, S, Lee KH, Lee HL, Proton conduction in La$_{0.6}$Ba$_{0.4}$ScO$_{2.8}$ cubic perovskite Solid State Ionics, **144** (2001) 109–115. https://doi.org/10.1016/S0167-2738(01)00887-6

28. Kato H, Kudo T, Naito H, Yugami H, Electrical conductivity of Al-doped La$_{1-x}$Sr$_x$ScO$_3$ perovskite-type oxides as electrolyte materials for low-temperature SOFC, Solid State Ionics, **159** (2003) 217–222. https://doi.org/10.1016/S0167-2738(03)00101-2

29. Stroeva AYu, Gorelov VP, Kuz'min AV, Antonova EP, Plaksin SV, Phase composition and conductivity of La$_{1-x}$Sr$_x$ScO$_{3-\alpha}$ (x = 0.01–0.20) under oxidative conditions, Russ. J. Electrochem., 48 (2012) 509–517. https://doi.org/10.1134/S1023193512050114

30. Kuzmin AV, Stroeva AYu, Gorelov VP, Novikova YuV, et al., Synthesis and characterization of dense proton-conducting La$_{1-x}$Sr$_x$ScO$_{3-\alpha}$ ceramics, Int. J. Hydrog. Energy, **44** (2019) 1130–1138. https://doi.org/10.1016/j.ijhydene.2018.11.041

31. Ricote S, Bonanos N, Manerbino A, Coors WG, Conductivity study of dense BaCe$_x$Zr$_{(0.9-x)}$Y$_{0.1}$O$_{(3-\delta)}$ prepared by solid state reactive sintering at 1500 °C, Int. J. Hydrog. Energy, **37** (2012) 7954–7961. https://doi.org/10.1016/j.ijhydene.2011.08.118

32. Medvedev DA, Murashkina AA, Demin AK, Formation of dense electrolytes based on BaCeO$_3$ and BaZrO$_3$ for application in solid oxide fuel cells: the role of solid-state reactive sintering, Rev. J. Chem., **5** (2015) 193–214. https://doi.org/10.1134/S2079978015030024

33. Loureiro FJA, Nasani N, Reddy GS, Munirathnam N.R., Fagg DP, A review on sintering technology of proton conducting BaCeO$_3$-BaZrO$_3$ perovskite oxide materials for protonic ceramic fuel cells, J. Power Sources, **438** (2019) 226991. https://doi.org/10.1016/j.jpowsour.2019.226991

34. Huang Y, Merkle R, Maier J, Effects of NiO addition on sintering and proton uptake of Ba(Zr,Ce,Y)O$_{3-\delta}$, J. Mater. Chem. A, **9** (2021) 14775–14785. https://doi.org/10.1039/D1TA02555D

35. Kuzmin AV, Lesnichyova AS, Tropin ES, Stroeva AYu, et al., LaScO$_3$-based electrolyte for protonic ceramic fuel cells: Influence of sintering additives on the transport properties and electrochemical performance, J. Power Sources, **466** (2020) 228255. https://doi.org/10.1016/j.jpowsour.2020.228255

36. Lesnichyova A, Belyakov S , Stroeva A , Petrova S, et al., Densification and proton conductivity of La$_{1-x}$Ba$_x$ScO$_{3-\delta}$ electrolyte membranes, Membranes, **12** (2022) 1084. https://doi.org/10.3390/membranes12111084

37. Farlenkov AS, Smolnikov AG, Ananyev MV, Khodimchuk AV, et al., Local disorder and water uptake in La$_{1-}$$_xSr_xScO_{3-\delta}$, Solid State Ionics, **306** (2017) 82–88. http://dx.doi.org/10.1016/j.ssi.2017.04.018

38. Lesnichyova A, Stroeva A, Belyakov S, Farlenkov A, et al., Water uptake and transport properties of La$_{1-x}$Ca$_x$ScO$_{3-\alpha}$ proton-conducting oxides, Materials, **12** (2019) 2219. https://doi.org/10.3390/ma12142219

39. Kreuer KD, Proton-conducting oxides, Annu. Rev. Mater. Res., **33** (2003) 333–359. https://doi.org/10.1146/annurev.matsci.33.022802.091825

40. Stroeva AYu, Balakireva VB, Dunyushkina LA, Gorelov VP, Electroconductivity and nature of ion transfer in La$_{1-x}$Sr$_x$Sc$_{1-y}$Mg$_y$O$_{3-\alpha}$ system (0.01 ≤ x = y ≤ 0.20) in dry and humid air, Rus. J. Electrochem., **46** (2010) 552–559 https://doi.org/10.1134/S1023193510050095

41. Okuyama Y, Kozai T, Ikeda S, Matsuka M, Sakai T, Matsumoto H, Incorporation and conduction of proton in Sr-doped LaMO$_3$ (M=Al, Sc, In, Yb, Y), Electrochim. Acta, **125** (2014) 443–449. http://dx.doi.org/10.1016/j.electacta.2014.01.113

42. Farlenkov AS, Putilov LP, Ananyev MV, Antonova EP, et al., Water uptake, ionic and hole transport in La$_{0.9}$Sr$_{0.1}$ScO$_{3-\delta}$, Solid State Ionics, **306** (2017) 126–136. https://doi.org/10.1016/j.ssi.2017.04.013

43. Kreuer KD, Adams St, Munch W, Fuchs A, et al., Proton conducting alkaline earth zirconates and titanates for high drain electrochemical applications, Solid State Ionics, **145** (2001) 295–306. https://doi.org/10.1016/S0167-2738(01)00953-5

44. Stroeva AY, Gorelov VP, Balakireva VB, Conductivity of La$_{1-x}$Sr$_x$Sc$_{1-y}$Mg$_y$O$_{3-\alpha}$ (x = y = 0.01–0.20) in reducing atmosphere, Russ. J. Electrochem., **46** (2010) 784–788. https://doi.org/10.1134/S1023193510070116

45. Gorelov VP, Stroeva AY, Solid proton conducting electrolytes based on LaScO$_3$, Russ. J. Electrochem., **48** (2012) 949–960. https://doi.org/10.1134/S1023193512100084

46. Islam MS, Slater PR, Tolchard JR, Dinges T, Doping and defect association in AZrO$_3$ (A = Ca, Ba) and LaMO$_3$ (M = Sc, Ga) perovskite-type ionic conductors, Dalton Transactions **19** (2004) 3061–3066. https://doi.org/10.1039/B402669C

47. Lesnichyova AS, Belyakov SA, Stroeva AYu, Kuzmin AV, Proton conductivity and mobility in Sr-doped LaScO$_3$ perovskites, Ceramics Int., **47** (2021) 6105–6113. https://doi.org/10.1016/j.ceramint.2020.10.189

48. Belyakov SA, Lesnichyova AS, Plekhanov MS, Prinz N, et al., Dopant-induced changes of local structures for adjusting the hydration ability of proton conducting lanthanum scandates, J. Mater. Chem. A, **11** (2023) 19605–19618. https://doi.org/10.1039/D3TA03673A

49. Kato H, Iguchi F, Yugami H, Compatibility and performance of La$_{0.675}$Sr$_{0.325}$Sc$_{0.99}$Al$_{0.01}$O$_3$ perovskite-type oxide as an electrolyte material for SOFCs, Electrochemistry, **82** (2014) 845–850. http://dx.doi.org/10.5796/electrochemistry.82.845

50. Iguchi F, Yamane T, Kato H, Yugami H, Low-temperature fabrication of an anode-supported SOFC with a proton-conducting electrolyte based on lanthanum scandate using a PLD method, Solid State Ionics, **275** (2015) 117–121. http://dx.doi.org/10.1016/j.ssi.2015.03.022

51. Plekhanov MS, Kuzmin AV, Tropin ES, Korolev DA, Ananyev MV, New mixed ionic and electronic conductors based on LaScO$_3$: Protonic ceramic fuel cells electrodes, J. Power

Sources, **449** (2020) 227476. https://doi.org/10.1016/j.jpowsour.2019.227476

52. Osinkin D, Tropin E, Hydrogen production from methane and carbon dioxide mixture using all-solid-state electrochemical cell based on a proton-conducting membrane and redox-robust composite electrodes, J. Energy Chem., **69** (2022) 576–584. https://doi.org/10.1016/j.jechem.2022.02.019